



ELSEVIER

Available online at [www.sciencedirect.com](http://www.sciencedirect.com)

Earth and Planetary Science Letters xx (2007) xxx – xxx

EPSL

[www.elsevier.com/locate/epsl](http://www.elsevier.com/locate/epsl)

# Valles Marineris landslides: Evidence for a strength limit to Martian relief?

Florence Bigot-Cormier\*, David R. Montgomery

*Quaternary Research Center and Department of Earth & Space Sciences, University of Washington, Seattle, WA 098195, United States*

Received 16 March 2007; received in revised form 11 May 2007; accepted 19 May 2007

Editor: T. Spohn

## Abstract

Unresolved controversies in Martian geology surround the role of active tectonics and a wetter climate early in Mars history, and particularly the history and amount of liquid water at or near the surface. Among the various lines of evidence brought into such debates are the massive landslides along the walls of Valles Marineris, which generally have been interpreted as resulting from marsquakes, and therefore necessitating active tectonics, under either wet or dry conditions. We analyze Valles Marineris landslides using digital elevation data from the Mars Orbiter Laser Altimeter (MOLA) and find that a relief limit consistent with the intact strength of evaporites or other weak sedimentary rock defines an upper bound to the length and relief of unfailed slopes, as would material with the strength properties of basalt lithology subjected to ground accelerations of about 0.2 g. In contrast to prior interpretations of Valles Marineris landslides, we propose an alternative, complementary hypothesis that does not require significant pore-water pressures or ground acceleration based on the close correspondence between back-calculated material strength properties and values consistent with portions of the chasm walls at least locally being composed of relatively weak materials, such as potentially frozen evaporites and/or mixtures of ash fall or flow deposits, ice, hydrated salts and lava flows.

© 2007 Published by Elsevier B.V.

*Keywords:* Mars; landslides; strength limit; climate; tectonics

## 1. Introduction

Large landslides have been observed on Mars since the Mariner 9 and Viking missions returned images of extraordinary slope failures associated with the deep canyons of Valles Marineris (Sharp, 1973; Christiansen and Head, 1978). Subsequent studies generally invoked marsquakes as the triggering agent for gigantic debris slides and flows and explained the occurrence, mor-

phology, and runout of these landslides by the presence of altered rock containing water or ice (Lucchitta, 1978, 1979, 1987; McEwen, 1989; Schultz, 2002; Soukhovitskaya and Manga, 2006). Ongoing debate about the stratigraphy of Valles Marineris centers on whether the valley walls are composed of stacked lava flows (McEwen et al., 1999; Schultz, 2002; Curasso, 2002) or relatively weak ash fall deposits potentially inter-stratified with evaporites and overlain by lava flows (Blaney and McChord, 1995; Forsythe and Zimbleman, 1995; Malin and Edgett, 2000; Feldman et al., 2004; Montgomery and Gillespie, 2005). Previous applications

\* Corresponding author.

*E-mail address:* [bigot@u.washington.edu](mailto:bigot@u.washington.edu) (F. Bigot-Cormier).

of a rock-mass rating system to measurements from MOLA-derived profiles of unfailed slopes were interpreted as showing that lava flows exposed in wallrock of Valles Marineris are stronger than the interior layered deposits (Schultz, 2002), which now have been spectrally determined to contain hydrated sulfates (Gendrin et al., 2005).

For terrestrial slopes, stability models using laboratory derived cohesion and friction angles of intact rock greatly overestimate the maximum stable relief of incised massifs because of the importance of pervasive discontinuities arising from weathering or tectonics that impart material or structural discontinuities to field-scale rock masses (Terzaghi, 1962; Carson and Kirkby, 1972). In general, the low strength of tectonically-induced discontinuities such as faults, joints, and inclined bedding surfaces reduces the bulk strength of rock at the scale of terrestrial mountains to well below values for intact rock samples (Hoek and Bray, 1997). Although small samples used in laboratory tests possess strength properties theoretically capable of supporting cliffs many kilometers high, the strength of terrestrial slopes is scale-dependent, with small samples of intact rock exhibiting uniaxial compressive strengths of 1 to

100 MPa and large rock masses typically exhibiting aggregate compressive strengths ranging from 0.1 to 1 Mpa, with the associated cohesion ( $C$ ) ranging from 0 (clay) to 0.7 MPa (schists, quartzites), and friction angles ( $\phi$ ) ranging from  $4.5^\circ$  (Montmorillonite clay) to  $45^\circ$  (granite) (Hoek and Bray, 1997).

## 2. Methodology

The simplest model for predicting the maximum stable height of a rock slope is the Culmann wedge model:

$$H_c = \frac{4C}{\rho g} \cdot \frac{\sin \beta \cdot \cos \theta}{[1 - \cos(\beta - \phi)]} \quad (1)$$

where  $H_c$  is the maximum limiting, or critical height, of the slope,  $\beta$  is the hillslope gradient,  $C$  is the cohesion,  $\rho$  is the bulk density,  $g$  is the gravitational acceleration, and  $\phi$  is the friction angle of the slope-forming material. Eq. (1) neglects, but can be modified to incorporate either pore-water pressure (Hoek and Bray, 1997) or seismic acceleration (Schmidt and Montgomery, 1995), which means that observed heights and slopes of

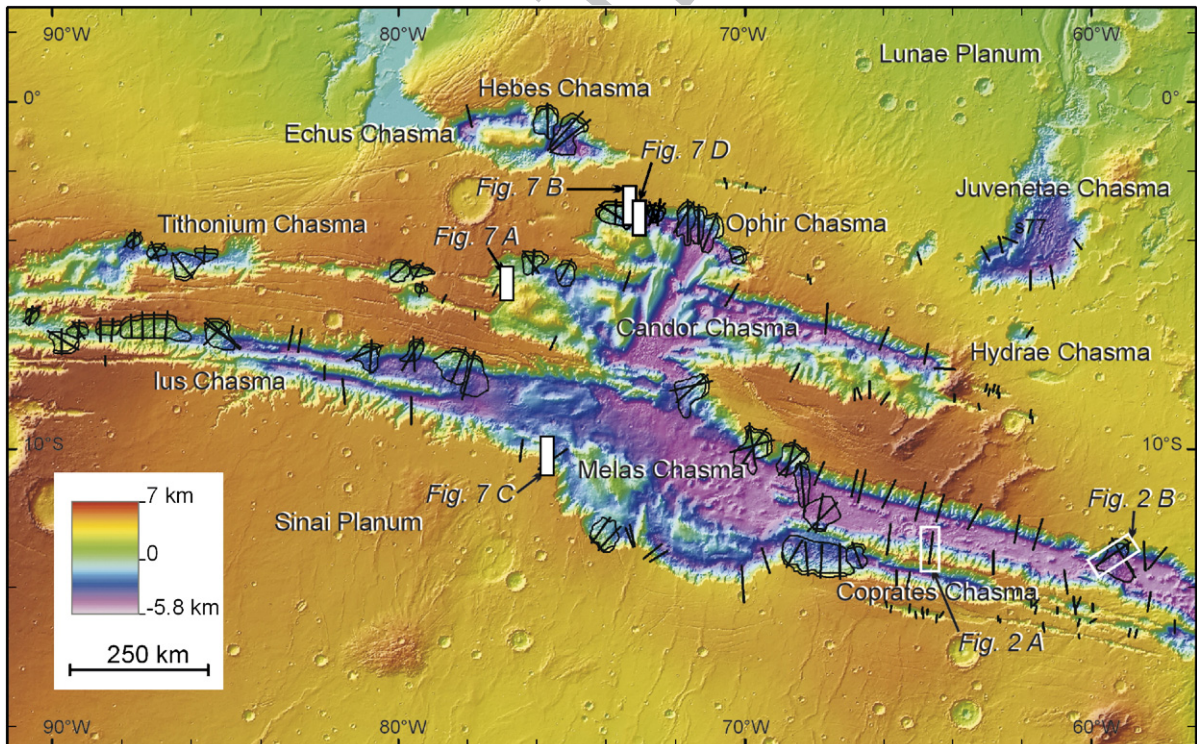


Fig. 1. Shaded relief map of the topography of Valles Marineris and vicinity showing the location of landslides and cross sections used in Figs. 2 and 3. Nominal grid size of digital elevation model is  $\sim 450$  m. The location of pictures from Fig. 7 is shown by white rectangles.

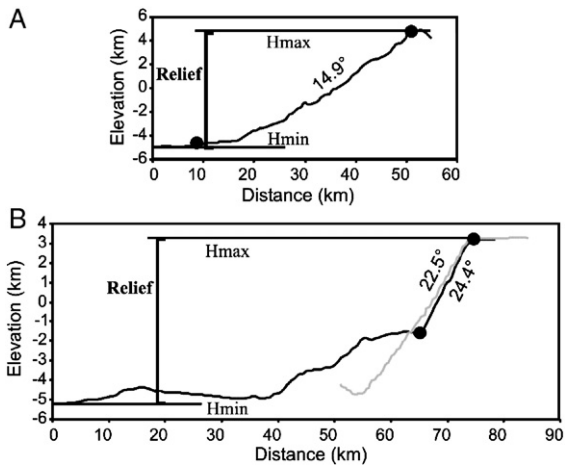


Fig. 2. Topographic profiles from (A) unfailed and (B) failed slopes illustrating the geometry of the analysis. Slope gradients were calculated between the base of scarp ( $X$ ) and the top of slope ( $Y$ ). Where possible the initial gradient for failed slopes was estimated by extrapolation from immediately adjacent unfailed slopes, as illustrated by grey line in panel B.

unfailed and failed hillslopes provide minimum constraints on back-calculated strength parameters, or the ground acceleration required to destabilize a rock slope of known material strength. More sophisticated models involving rotational failure geometries require additional assumptions about unobservable subsurface conditions. Although this limits the utility of the Culmann model for engineering purposes, it has been widely used in geomorphological studies to empirically constrain outcrop and landscape scale ranges of effective bulk-scale  $C$  and  $\phi$  values for use in predicting the maximum unfailed height of slopes ranging in scale from stream banks and gully heads (Skempton, 1953; Lohnes and Handy, 1968) to the relief of terrestrial mountains (Schmidt and Montgomery, 1995). Using Eq. (1), measurements of the slope and height (relief) of both unfailed and failed valley walls can bracket minimum and maximum estimates of the calibrated bedrock material strength, and thereby define a maximum stable relief (MSR) uniquely proscribed by particular combinations of back-calculated  $C$  and  $\phi$  that incorporate both scaling effects and assumptions inherent to the model.

Despite its simplistic geometry, Schmidt and Montgomery (1995) found back-calculated  $C$  and  $\phi$  values for an empirical MSR fit to data from large landslides in the Northern Cascade Range and the Santa Cruz Mountains to be close to those measured *in situ* on outcrop-scale planes of weakness and discontinuities—but dramatically lower than for laboratory-derived values from small intact rock samples. As the landslides

mapped by Schmidt and Montgomery (1995) included large rotational slumps, the close correspondence between back-calculated and measured  $C$  and  $\phi$  values they reported indicates that the simple Culmann model can provide a useful approximation of more complex conditions. Subsequently, a number of empirical and theoretical studies provided evidence for the development of threshold slopes that limit the relief of terrestrial hillslopes and valley walls (Burbank et al., 1996; Roering et al., 1999; Montgomery, 2001; Montgomery and Brandon, 2002).

We analyzed 36 large landslides throughout Valles Marineris using MOLA digital elevation data (Fig. 1). These mapped landslides account for all identifiable landslides in the study area that we found resolvable on the MOLA digital elevation data (0.45 km/pixel) (Smith et al., 2001), including the subset of those mapped previously by Quantin et al. (2004) that are in the study area. Analysis of finer-scale Mars Orbiter Camera (MOC;  $\geq 2$  m/pixel resolution) and the Mars Express High-Resolution Stereo Camera (HRSC;  $\geq 10$  m/pixel resolution) images (Smith et al., 2001; Malin and Edgett, 2001; Christensen et al., 2004) reveals additional smaller landslides not resolvable by the MOLA digital elevation data, and thus not analyzed here.

We constructed 64 distance-versus-elevation profiles from the failed slopes resolvable by MOLA data in and proximal to Valles Marineris, acquiring one to four

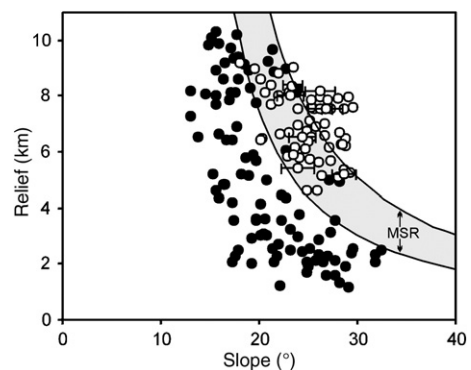


Fig. 3. Gradient versus relief for unfailed hillslopes (●) and landslide sites (○) in Valles Marineris. Grey shading represents the envelope fit by eye using Eq. (1) to the lower bound of data from failed slopes and the upper bound of data from unfailed slopes. Material properties back calculated from these fitted relations using Eq. (1) with  $g=3.72 \text{ m s}^{-2}$  and the bulk density of gypsum ( $\rho=2300 \text{ kg m}^{-3}$ ) and basalt ( $\rho=3300 \text{ kg m}^{-3}$ ) yielded  $\phi=9$  for both lithologies and respective  $C$  values for the lower and upper curves of 0.9 MPa and 1.2 MPa for gypsum and 1.5 MPa to 2.1 MPa for basalt. Error bars represent range of slope estimates for failed slopes where the high end of the range represents the post-failure scarp and the low end represents the slope extrapolated from neighboring unfailed slopes.

147 profiles for each landslide depending on its size and  
 148 geometry. Pre-failure relief was estimated from the  
 149 elevation difference between the unfailed plateau  
 150 surface at the head of each slide and the chasm bottom  
 151 immediately beyond the bounds of the slide deposit.  
 152 Pre-failure slopes were approximated from neighboring  
 153 unfailed slopes where such an extrapolation reasonably  
 154 could be made, and by the slope of the slide headscarp to

155 provide a limiting upper bound where no other local  
 156 constraint was justified (Fig. 2). We also obtained 101  
 157 additional profiles of unfailed slopes to estimate the  
 158 relief and slope gradient for stable, unfailed valley walls.  
 159 We fit an MSR limit based on Eq. (1) to both the upper  
 160 envelope of the data for unfailed slopes (upper limit on  
 161 Fig. 3) and the lower envelope of data for failed slopes  
 162 (lower limit on Fig. 3).

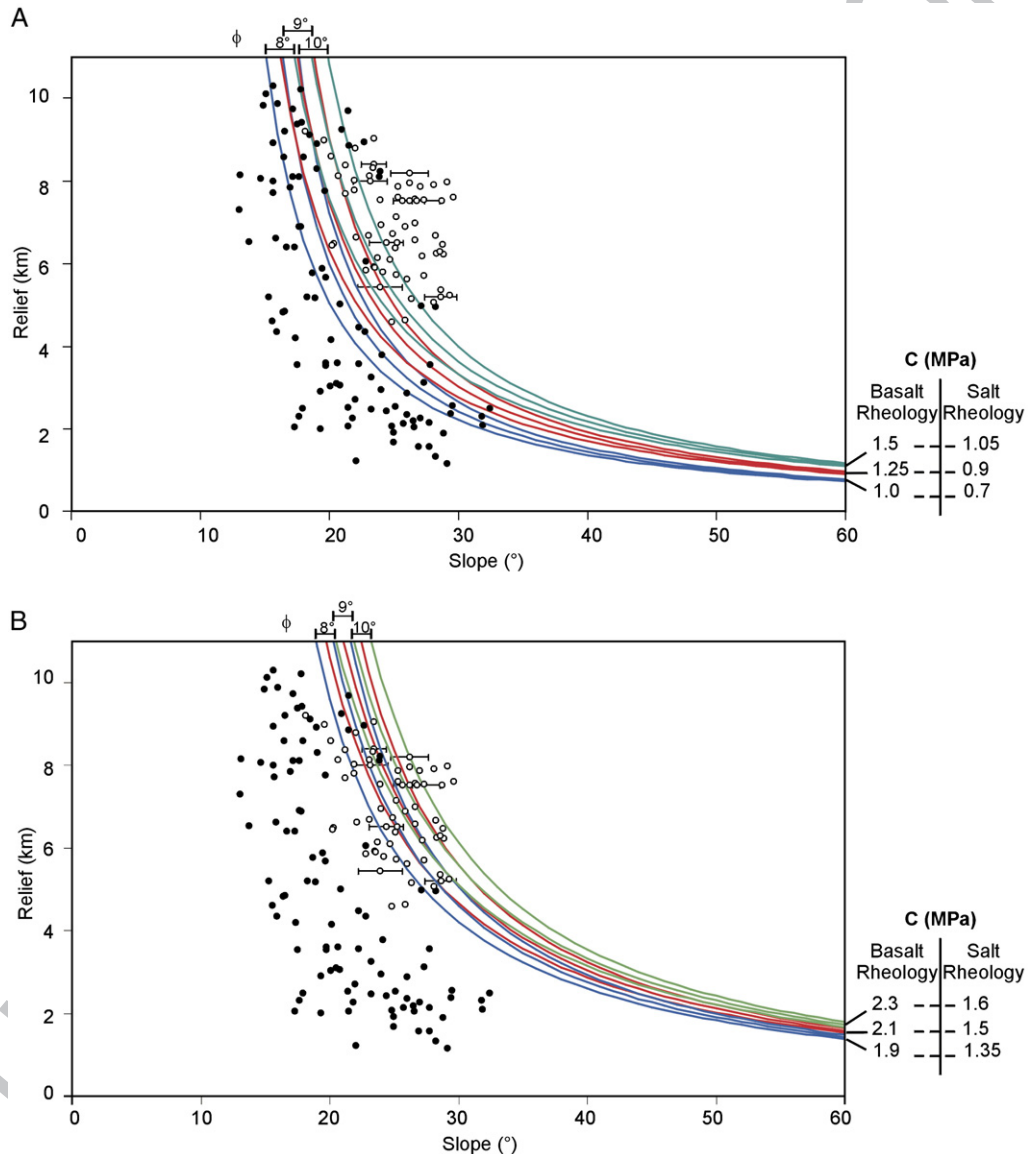


Fig. 4. Illustration of the method for determining the maximum stable relief (MSR) bound for the lower limit (A) for basalt and evaporite then for the upper limit (B) by calculating successively  $C$  and  $\phi$ . Different values of  $C$  are characterized by different colors with  $\phi$  varying according to the  $C$  value; hence each first line of each color correspond to  $\phi=8^\circ$ , each second line of each color correspond to  $\phi=9^\circ$  and the last line of each color is  $\phi=10^\circ$ ; note that values which reasonably separate data from stable and unstable slopes lie between  $C=0.7$  and  $1.5$  MPa for the lower limit and between  $C=1.35$  and  $2.3$  MPa for the upper limit with  $\phi=8-10^\circ$ .

### 163 3. Results

164 In general, the initial (i.e., pre-failure) slope of a site  
 165 of a given height is steeper than stable slopes of  
 166 comparable height (Fig. 3). Unfailed hillslopes with  
 167 gradients between 15 and 20° reach more than 10-km  
 168 height, but few hillslopes with gradients >32° rise more  
 169 than 1 km. As the boundary between data from unfailed  
 170 and failed slopes in Fig. 3 is transitional, the two MSR  
 171 curves that define the upper and lower limits on Fig. 3  
 172 bracket the range of back calculated  $C$  and  $\phi$  values that  
 173 are consistent with an arcuate upper bound character-  
 174 izing the maximum unfailed topographic relief in Valles  
 175 Marineris. As the back-calculated values of  $C$  depend  
 176 on the bulk density of the slope-forming material, we  
 177 used end-member values to constrain back-calculated  
 178 material strength properties for each curve based on the  
 179 density of either basalt ( $\rho=3300 \text{ kg m}^{-3}$ ) or gypsum  
 180 ( $\rho=2300 \text{ kg m}^{-3}$ ). The MSR fit to the two curves by  
 181 successive approximations yields strength values rang-  
 182 ing from  $C=0.7$  to 2.3 MPa and with  $\phi=8\text{--}10^\circ$  (Fig. 4).  
 183 Inclusion of seismic acceleration in the analysis reveals  
 184 that a comparable MSR can be fit to the same data using  
 185 either the density of gypsum or the density of basalt with  
 186 a 0.2 g acceleration (Fig. 5). Hence, either low density or  
 187 a modest acceleration produce similar fits to the lower  
 188 bound of the MSR.

189 Many of the topographic profiles through landslides  
 190 show evidence for a complex morphology indicative of  
 191 an initial translational or slump failure and a longer run  
 192 out zone composed of apparently fluidized material  
 193 originating in the initial slump zone. In addition, such  
 194 profiles often exhibit a distinct break in slope coincident  
 195 with the landslide headscarp (Fig. 6), suggesting that

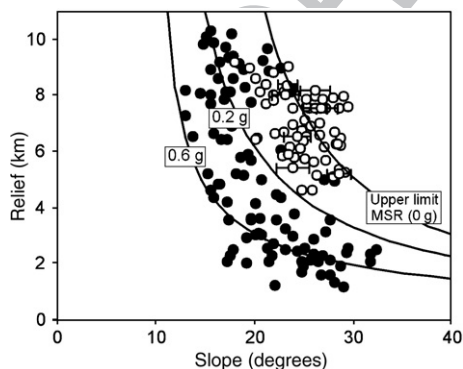


Fig. 5. Same data as shown in Fig. 3, but with MSR also calculated for 0.6 g and 0.2 g ground acceleration, assuming a wall only constituted by basalt ( $\rho=3300 \text{ kg m}^{-3}$ ) and the back-calculated bulk-scale strength properties for the upper limit to the MSR shown in Fig. 3 (i.e., 2.1 MPa and  $\phi=9^\circ$ ).

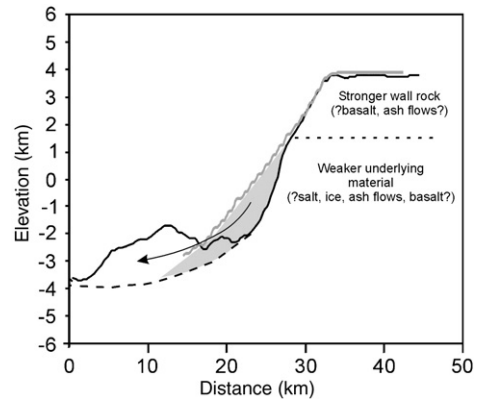


Fig. 6. Example of failed slope showing common pattern of a prominent break in slope coincident with the landslide headscarp location several kilometers below the rim of Valles Marineris, suggestive of a material discontinuity within the wall rock as speculatively illustrated for this example and further illustrated in Fig. 7. Gray line shows profile of neighboring unfailed slope, which provides a reasonable approximation for the shape of the pre-failure slope.

initial failures involved the lower portions of the 196 exposed valley wall. 197

### 198 4. Discussion 199

200 There is a substantial difference between material 201 properties back-calculated for the walls of Valles 202 Marineris and those for terrestrial slopes, where large- 203 scale back-calculated cohesion values are on the order of 204 26–150 kPa (Schmidt and Montgomery, 1995), one to 205 two orders of magnitude smaller than similarly back- 206 calculated values for Valles Marineris (0.9–2.1 MPa). 207 This could reflect greater innate strength of the Martian 208 slope-forming material due, for example, to fewer 209 material or structural discontinuities. This interpretation 210 is supported by similarity between back-calculated 211 cohesion on the order of MPa for the immense slopes 212 of Valles Marineris and uncalibrated laboratory values 213 for intact samples of weak sedimentary rock (Hoek and 214 Bray, 1997).

215 In contrast, the low back-calculated  $\phi$  values in- 216 dicated by our analysis for Valles Marineris are roughly 217 half the lowest values back-calculated from large-scale 218 terrestrial applications of Eq. (1) (Schmidt and Mon- 219 tomy, 1995). Moreover, they are well below the 220 typical limiting gradient (and hence friction angle) of 221 30–35° for terrestrial relief (Montgomery, 2001; 222 Montgomery and Brandon, 2002). However, the 223 unusually low back-calculated  $\phi$  values lie within the 224 5–18° range of friction angles estimated by Schultz 225 (2002) for the interior layered deposits that outcrop in 226 Valles Marineris, which others (Malin and Edgett, 2000; 227

226 Montgomery and Gillespie, 2005) have argued represent  
 227 exhumed deposits that, at least locally, compose a  
 228 portion of the stratigraphy exposed in the walls of Valles  
 229 Marineris. Schultz (2002) also coupled measurements  
 230 from MOLA and a Rock Mass Rating system (RMR) to

compare the RMR values from Earth to those obtained 263  
 for Valles Marineris and interpreted that the walls of 264  
 Valles Marineris were composed of fractured basaltic 265  
 rock, a conclusion consistent with the global basaltic 266  
 compositions of Mars obtained by spectral observations 267  
 from the Thermal Emission Spectrometer (Bandfield 268  
 et al., 2000). 269

Our analysis shows that an MSR can be fit to the 270  
 observed data using either low rock strength or modest 271  
 ground acceleration, which could potentially result from 272  
 impact events after formation of Valles Marineris. 273  
 Hence, while it is likely that marsquakes could impact 274  
 slope stability in Valles Marineris, as already demon- 275  
 strated by others (Schultz, 2002; Neuffer and Schultz, 276  
 2006), such events would not be required to explain 277  
 failure of chasm walls of low rock strength. 278

This view is supported at another scale by Gendrin 279  
 et al.'s (2005) report of spectral evidence for sulfate 280  
 salts–gypsum and kieserite–associated with light-toned 281  
 layered deposits in Valles Marineris. Malin and Edgett 282  
 (2001) interpreted such deposits in Valles Marineris as 283  
 ancient sedimentary rocks that, at least locally, underlay 284  
 the surface-forming lava flows that at least in places 285  
 appear to form the entire section from chasm top to 286  
 bottom (McEwen et al., 1999). Although many workers 287  
 subscribe to the alternative view that the interior layered 288  
 deposits formed *within* Valles Marineris, and were thus 289

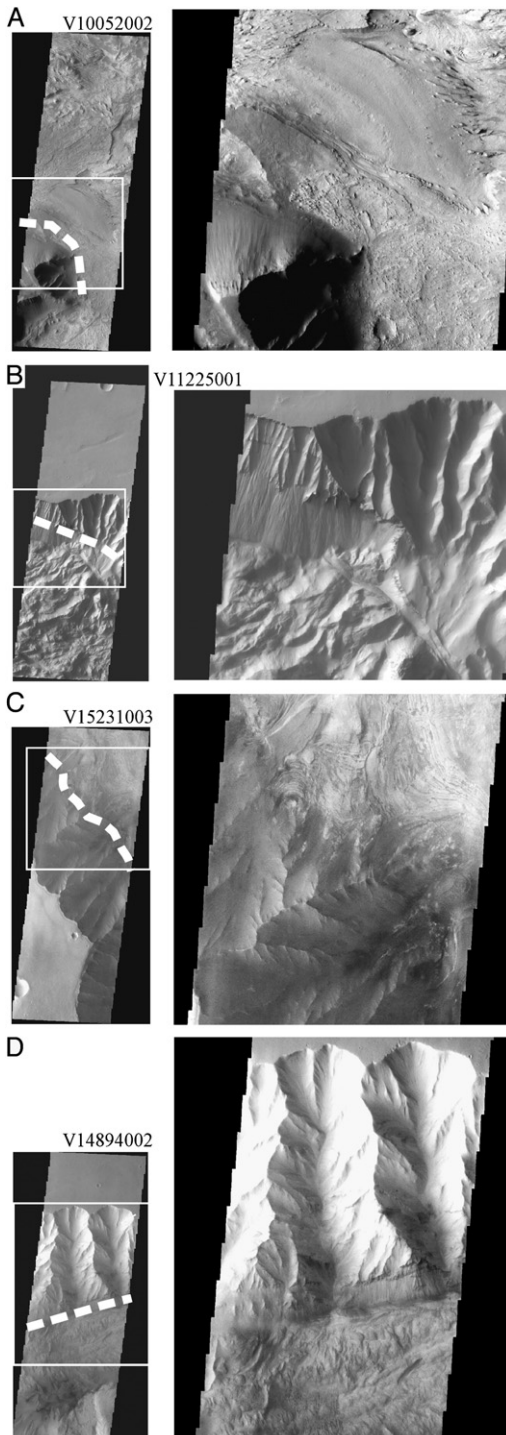


Fig. 7. Themis images showing evidence of stratigraphic variability consistent with different relative vertical positions of a potentially weaker formation exposed in the wall of Valles Marineris beneath the planum-forming lava flows. Full images shown on left; white boxes indicate areas shown as enlargements on right. Thick white lines in images on left indicate approximate locations of stratigraphic contacts. Slant distance on full images is 400 km; pixel resolution is 18 m. (A) V10052002 showing a stable slope in west Candor Chasma that reaches from the top of the planum in the lower left of enlargement to the Chasma floor in the center of the enlargement. Note the continuous exposure of wall-forming materials down the slope and the transition from the steep, dark upper wall to the light-toned layered outcrops on the lowest portions of the slope. (B) V11225001 showing evidence for a lithologic contact in the wall of Ophir Chasma running from upper left to lower right of enlargement. Rocky, ridge-forming material extends from planum surface to the contact partway down both the failed (left) side of image, where contact is higher in the section, and unfailed (right) portions of the slope, where the contact is lower on the slope. In particular, note how both failed and unfailed slopes are smoother below the contact. (C) V15231003 showing wall of Melas Chasma from planum surface to the chasma floor. Note that the upper portions of the chasm wall are composed of ridge-forming material that gives way to light-toned layered outcrops in the lower valley wall. (D) V14894002 showing rocky ridge-forming material extending most of the way down a stable slope on the wall of Candor Chasma and potential contact between ridge-forming material and smoother material near the base of the wall section.

deposited after rather than before incision of the chasm, Montgomery and Gillespie (2005) and Catling et al. (2006) recently provided further evidence that light-toned layered deposits outcrop in the walls of Valles Marineris and Juventae Chasma. It is possible that thick accumulations of hydrated salts originally deposited in Noachian craters and basins, such as those examined by the Mars Rover Spirit at Gusev Crater (Squyres et al., 2004), were buried by the Hesperian lava flows that cap the section at Valles Marineris. If now exposed in the walls of the chasm, such laterally unconfined exposures of salts, or frozen mixtures of salt and ice, could result in ductile flow such as observed in terrestrial salt glaciers (Talbot and Rogers, 1980; Jackson and Talbot, 1986) and eventually trigger slope instability, particularly if loaded from overlying lava flows and exposed along unconfined faces in valley walls. Consequently, and whatever the age of this weak materials, we hypothesize that many of the spectacular failures of the walls of Valles Marineris are related to exposure of relatively weak materials in the valley walls and we further suggest that the low  $\phi$  back-calculated from failed slopes could reflect the presence of weak materials within the local stratigraphy of the failed slopes, such as the light-toned layered deposits previously interpreted to outcrop in the valley-walls (Malin and Edgett, 2000; Montgomery and Gillespie, 2005; Catling et al., 2006). Examination of additional Themis images of stable and failed slopes around Valles Marineris revealed evidence for spatial variability in the proportion of the relief of the valley walls composed of potentially weaker materials (Fig. 7), which may help to explain the anomalously low back-calculated friction angles found in our analysis of failed slopes.

Our analysis does not refute the hypothesis that pore-water pressures contributed to instability of the valley walls, although the presence of water as a liquid phase would promote slope instability and should lead to lower effective  $C$  values more like those back-calculated for Earth than those we find for Mars. Neither does our analysis rule out a role for active tectonics nor continued cratering after incision of Valles Marineris in triggering slope instability. However, the apparent role of material strength on limiting the unfailed relief along Valles Marineris challenges the basis for inferences based on past interpretations that large Martian landslides necessarily record a history of either wetter conditions or active seismicity. Although marsquakes would be an effective mechanism to destabilize steep slopes, our results show that the chasmata of Valles Marineris are already incised to close to the height potentially supportable by relatively weak deposits, such as the

evaporites for which there are independent reasons to suspect may characterize at least local portions of the regional stratigraphy.

Still, the extreme view of triggering slope failure simply through incision of Valles Marineris would imply that the landslides formed soon after incision of the chasm, roughly 3.5 billion years ago. Recently Quantin et al. (2004) interpreted the slides to be an ongoing process based on crater-count estimated ages of slides in and around Valles Marineris that ranged from 60 million to 3.5 billion years, essentially the full time span since the formation of the chasm. Ground acceleration due to proximal impact events could provide a mechanism for triggering landslides long after chasm formation. However, if slides are composed of mechanically weak rock subjected to sand-charged winds, such as would be expected within Valles Marineris, it would challenge the implicit assumption of no erosion on cratered surfaces, making inferred crater-count ages date an evolving surface age, and therefore constrain the erosion rate rather than the formation age.

Following Soukhovitskaya and Manga (2006), we also interpret evidence for fluidized flow in the slide runout areas as not requiring the influence of initially high pore-water pressures in the valley walls. Instead we consider the apparent fluidity of the distal ends of large slumps of Valles Marineris (Lucchitta, 1978, 1979, 1987) as more likely due to frictional heating that either melts entrained ice (Harrison and Grimm, 2003) or dewateres evaporites (Montgomery and Gillespie, 2005) during failure and runout of the landslides. Although our analysis sheds no light on the problem of how the chasmata were carved in the first place, we conclude that the immense landslides of Valles Marineris do not provide compelling *a priori* evidence of either active tectonics or warm/wet conditions in the Martian past, as they previously have been interpreted as doing. Instead, we propose the alternative, although not mutually exclusive, hypothesis that many of these gigantic landslides reflect exposure of unusually weak materials in the valley walls. We further suggest that the local presence or absence of this weak material and the relative elevation to which it crops out on the valley walls (i.e., whether the contact is closer to the top or the bottom) may exert a profound local influence on the stability of the chasmata walls.

## Acknowledgments

We thank Alan Gillespie, David Catling, John Adams, Sanjoy Som, Stephen Wood, and Conway Leovy for stimulating discussions about the geology of Mars. We

392 also thank Victor Baker, Taylor Perron, two anonymous  
393 reviewers, and the late Richard Stewart for their  
394 comments on draft manuscripts. This work was supported  
395 in part by NASA Mars Data Analysis Program Grant  
396 NNG04GK42G.

## 397 References

398 Bandfield, J.L., Hamilton, V.E., Christensen, P.R., 2000. A global view  
399 of Martian surface compositions from MGS-TES. *Science* 287,  
400 1626–1630.  
401 Blaney, D.L., McChord, T.B., 1995. Indications of sulfate minerals in the  
402 Martian soil from Earth-based spectroscopy. *J. Geophys. Res.* 100,  
403 14,433–14,441.  
404 Burbank, D.W., Leland, J., Fielding, E., Anderson, R.S., Brozovic, N.,  
405 Reid, M.R., Duncan, C., 1996. Bedrock incision, rock uplift and  
406 threshold hillslopes in the northwestern Himalayas. *Nature* 379,  
407 505–510.  
408 Carson, M.A., Kirkby, M.J., 1972. *Hillslope Form and Process*.  
409 Cambridge University Press, London, p. 475.  
410 Catling, D.C., Wood, S.E., Leovy, C., Montgomery, D.R., Greenberg,  
411 H.M., Glein, C.R., Moore, J.M., 2006. Light-toned layered  
412 deposits in Juventae Chasma, Mars. *Icarus* 181, 26–51.  
413 Christensen, P.R., et al., 2004. The Thermal Emission Imaging System  
414 (THEMIS) for the Mars 2001 Odyssey mission. *Space Sci. Rev.*  
415 110, doi:10.1023/B:SPAC.0000021008.16305.94.  
416 Christiansen, E.H., Head, J.W., 1978. Martian landslides—classifica-  
417 tion and genesis: reports of Planetary Geology Programs, 1977–  
418 1978. NASA Tech. Memo. 79729, 285–287.  
419 Curasso, P.A. (2002) Seismic triggering of Martian landslides and  
420 slope stability for Valles Marineris, Mars [M. S. thesis]: Reno,  
421 University of Nevada pp. 92.  
422 Feldman, W.C., Mellon, M.T., Maurice, S., Prettyman, T.H., Carey, J.W.,  
423 Vaniman, D.T., Bish, D.L., Fialips, C.I., Chipera, S.J., Kargel, J.S.,  
424 Elphic, R.C., Funsten, H.O., Lawrence, D.J., Tokar, R.L., 2004.  
425 Hydrated states of MgSO<sub>4</sub> at equatorial latitudes on Mars. *Geophys.*  
426 *Res. Lett.* 31, L16702, doi:10.1029/2004GL020181.  
427 Forsythe, R.D., Zimbelman, J.R., 1995. A case for ancient evaporite  
428 basins on Mars. *J. Geophys. Res.* 100, 5553–5563.  
429 Gendrin, A., Mangold, N., Bibring, J.P., Langevin, Y., Gondet, B.,  
430 Poulet, F., Bonello, G., Quantin, C., Mustard, J., Arvidson, R.,  
431 LeMouelic, S., 2005. Sulfates in martian layered terrains: the  
432 OMEGA/Mars Express view. *Science* 307, 1587–1591.  
433 Harrison, K.P., Grimm, R.E., 2003. Rheological constraints on martian  
434 landslides. *Icarus* 163, 347–362.  
435 Hoek, E., Bray, J., 1997. *Rock Slope Engineering*. The Institution of  
436 Mining and Metallurgy, London, p. 402.  
437 Jackson, M.P.A., Talbot, C.J., 1986. External shapes, strain rates, and  
438 dynamics of salt structures. *Geol. Soc. Amer. Bull.* 97, 305–323.  
439 Lohnes, R.A., Handy, R.L., 1968. Slope angles in friable loess. *J. Geol.*  
440 76, 247–258.  
442

Lucchitta, B.K., 1978. A large landslide on Mars. *Geol. Soc. Amer.* 441  
442 *Bull.* 89, 1601–1609.  
Lucchitta, B.K., 1979. Landslides in Valles Marineris, Mars. 443  
444 *J. Geophys. Res.* 84, 8097–8113.  
Lucchitta, B.K., 1987. Valles Marineris, Mars: wet debris flows and 445  
446 ground ice. *Icarus* 72, 411–429.  
Malin, M.C., Edgett, K.S., 2000. Sedimentary rocks of early Mars. 447  
448 *Science* 290, 1927–1937.  
Malin, M.C., Edgett, K.S., 2001. Mars Global Surveyor Mars Orbiter 449  
450 Camera. Interplanetary cruise through primary mission. *J. Geophys.*  
451 *Res.* 106 (E10), 23,429–23,570, doi:10.1029/2000JE001455.  
McEwen, A.S., 1989. Mobility of large rock avalanches: evidence 452  
453 from Valles Marineris, Mars. *Geology* 17, 1111–1114.  
McEwen, A.S., Malin, M.C., Carr, M.H., Hartmann, W.K., 1999. 454  
455 Voluminous volcanism on early Mars revealed in Valles Marineris.  
456 *Nature* 397, 584–586.  
Montgomery, D.R., 2001. Slope distributions, threshold hillslopes and 457  
458 steady-state topography. *Am. J. Sci.* 301, 432–454.  
Montgomery, D.R., Brandon, M.T., 2002. Non-linear controls on 459  
460 erosion rates in tectonically active mountain ranges. *Earth Planet.*  
461 *Sci. Lett.* 201, 481–489.  
Montgomery, D.R., Gillespie, A., 2005. Formation of Martian outflow 462  
463 channels by catastrophic dewatering of evaporite deposits. *Geology* 33,  
464 625–628.  
Neuffer, D.P., Schultz, R.A., 2006. Mechanisms of slope failure in Valles 465  
466 Marineris, Mars. *Quarter J. Eng. Geol. Hydrogeol.* 39, 227–240.  
Quantin, C., Allemand, P., Mangold, N., Delacourt, C., 2004. Ages of 467  
468 Valles Marineris (Mars) landslides and implications for canyon  
469 history. *Icarus* 172, 555–572.  
Roering, J.J., Kirchner, J.W., Dietrich, W.E., 1999. Evidence for 470  
471 nonlinear, diffusive sediment transport on hillslopes and implica-  
472 tions for landscape morphology. *Water Resour. Res.* 35, 853–870.  
Schmidt, K.M., Montgomery, D.R., 1995. Limits to relief. *Science* 473  
474 270, 617–620.  
Schultz, R.A., 2002. Stability of rock slopes in Valles Marineris, Mars. 475  
476 *Geophys. Res. Lett.* 29, 1932, doi:10.1029/2002GL015728.  
Sharp, R.P., 1973. Mars: Troughed terrain. *J. Geophys. Res.* 78, 477  
478 4063–4073.  
Skempton, W., 1953. Soil mechanics in relation to geology. *Proc.* 479  
480 *Yorks. Geol. Soc.* 29, 33–62.  
Smith, D.E., et al., 2001. Mars Orbiter Laser Altimeter: experiment 481  
482 summary after the first year of global mapping of Mars. *J. Geophys.*  
483 *Res.* 106 (E10), 23,689–23,722, doi:10.1029/2000JE001364.  
Soukhovitskaya, V., Manga, M., 2006. Martian landslides in Valles 484  
485 Marineris: wet or dry? *Icarus* 180 (2), 348–352.  
Squyres, S.W., et al., 2004. In situ evidence for an ancient aqueous 486  
487 environment at Meridiani Planum, Mars. *Science* 306, 1709–1714.  
Talbot, C.J., Rogers, E.A., 1980. Seasonal movements in a salt glacier 488  
489 in Iran. *Science* 208, 395–397.  
Terzaghi, K., 1962. Stability of steep slopes on hard unweathered rock. 490  
491 *Géotechnique* 12, 251–270.